ISSN: 0973-4929, Vol. 15, No. (1) 2020, Pg. 137-150

Current World Environment

www.cwejournal.org

Solar Light Induced Photocatalysis for Treatment of High COD Pharmaceutical Effluent with Recyclable Ag-Fe Codoped TiO_2: Kinetics of COD Removal

DARSHANA TUSHAR BHATTI[1]* and SACHIN PRAKASHBHAI PARIKH[2]

[1]Department of Chemical Engineering, VVP Engineering College affiliated to Gujarat Technological University, Rajkot, Gujarat, India.
[2]Department of Chemical Engineering, L.D. College of Engineering affiliated to Gujarat Technological University, Ahmedabad, Gujarat, India.

Abstract

A wide range of active pharmaceutical ingredients (API) is found in various water streams. These synthetic non-biodegradable organics create trouble in conventional wastewater treatment due to toxicity. There is a strong need to develop substitute technology such as visible light driven photocatalysis with a reusable photocatalyst to completely oxidize these substances into carbon dioxide and water. Sol-gel method was used for synthesis of Fe doped TiO_2 and Ag-Fe codoped TiO_2 nanoparticles with 0.5 wt% Fe and Ti/Ag molar ratio 30 (Ag-Fe CT 30). The morphology and structure of nanoparticles were studied using various analytical techniques. Ag-Fe CT 30 photocatalyst has exhibited excellent photocatalytic activity compared to commercial TiO_2, undoped TiO_2 and Fe doped TiO_2 nanophotocatalysts under solar and UV irradiation for removal of an antifungal drug intermediate, Difloro triazole acetophenone (DFTA) from water. COD reduction efficiency was highest with Ag-Fe CT 30 under solar and UV irradiation proves the potential of Ag-Fe CT 30 photocatalyst to absorb both UV as well as visible radiations. Ag-Fe CT 30 has shown good stability for 4 runs without much decline in the efficacy. This study provides insights on the solar application of a reusable Ag-Fe CT 30 photocatalyst for the treatment of high strength COD wastewater. Kinetics of COD reduction by photocatalysis has been determined.

Article History

Received: 16 March 2020
Accepted: 18 April 2020

Keywords

Ag-Fe Co-doped TiO_2,
Difloro Triazole Acetophenone,
Recyclability,
Solar Photocatalysis

Introduction

Environmental pollution and energy shortages have become the major sectors restricting progress and economical development of the country.[1–4] Some researchers have explored nowadays various solar applications for simultaneous solar

CONTACT Darshana Tushar Bhatti darshana333@yahoo.com Department of Chemical Engineering, VVP Engineering College affiliated to Gujarat Technological University, Rajkot, Gujarat, India.

Doi: http://dx.doi.org/10.12944/CWE.15.1.17

fuel cells and photocatalysis using iron-graphene oxide-titanium phosphate,ss[5] photocatalysis with cadmium sulphide,[6] transition metals doped CuO for heterojunction solar cells,[7] carbon nanotubes on cobalt-iron-silica electrocatalysis.[8] Active pharmaceutical ingredients (API) are the pollutants those come out from many pharmaceutical industries and pose major threats when disposed on to either land or in water bodies, as many of these refractory organics are toxic.[9] Conventional wastewater treatment has two drawbacks: 1) it is unable to biodegrade these refractory organics in activated sludge process unit; 2) it will just transfer pollutants from wastewater to solid phase as sludge, again there will be a disposal problem leading to solid pollution. Hence, there is a strong need to develop certain alternative treatment technologies which will completely oxidize these organics. Heterogeneous photocatalysis treatment using titanium dioxide (TiO_2) nanoparticles, generate hydroxyl radicals (OH*) which has the strong oxidizing potential of 2.8 eV,[10] and is a promising technology to degrade organics present in effluent competently.[11] The limitation of the treatments are: 1) it absorbs only UV radiations due to higher band gap ofTiO_2 [12] and 2) feasibility for reuse of the photocatalyst after treatment; which has limited the practical application of this treatment on filed.[13] Solar photocatalysis imbibing sustainable use of resources with economic and environmental benefits. One most important aspect to be considered for photocatalysis is recyclability which remains untouched by researchers.[12,14] For economic application of the photocatalyst, it should be recycled after use without sacrificing COD removal efficiency. It is generally observed that photocatalysts deactivation take place mainly due to adsorption of organics on the surface of a catalyst which cause poisoning catalysts. In development of a photocatalyst, its surface should be such that less poison occurs which makes it reusable for many cycles efficiently.[6-7] Many researchers have worked on synthesis, morphology and optical properties improvement by doping.[17-19] Some researchers have worked on photocatalysis using immobilized TiO_2 such as nanotube,[20] nanofilm[21-22] and nanowire[23] which can be less poisoned compared to nanopowders from treated water; but these structures will provide less surface area compared to suspended catalysts. At present, only few research focused on the recyclability of photocatalysts[8-10] which is one of the desired properties. The objective of this research was to develop novel Ag-Fe codoped TiO_2 nanoparticles that would facilitate a quick degradation of DFTA in solar radiation and simultaneously shows good stability over the number of recycling runs. This research also addressed kinetics of COD removal for solar and UV photocatalysis. There has been found less literature on doping with silver[11-12] and iron[11-12] in TiO_2 to enhance its activity under solar irradiations for pharmaceutical effluent treatment with high COD (75000 mg/L). In the present investigation TiO_2, Fe doped TiO_2 and Ag-Fe Codoped TiO_2 nanoparticles were synthesized using sol-gel method[29] and used for the photodegradation of DFTA from aqueous solution under optimized conditions of pH, catalyst dose and Ti/Ag molar ratio by prior experiments. The rate of photocatalysis was studied in terms of COD removal efficiency using TiO_2, Fe DT and Ag-Fe CT 30 which was finally compared with commercially available TiO_2 under solar and UV radiations Recyclability of novel photocatalyst has been determined. The applicability of novel Ag-Fe CT 30 was checked for treatment of high strength industrial pharmaceutical effluent at optimum conditions to remove COD and NH_3-N.

Experimental

Materials

Titanium (IV) tetraisopropoxide (TTIP)-97% and TiO_2 (Degussa P25)-99.5% were purchased from Sigma–Aldrich. Nitric acid-100%, isopropyl alcohol (IPA)-97%, ferric nitrate-99.95% and silver nitrate-99% were purchased from the Merck. Caustic soda-97% and sulphuric acid-99.99% were used to maintain the pH of the solution during experiments. DFTA was provided by Endoc lifecare private limited. All these chemicals were used without further purification. Distilled water was used to prepare all the solutions.

Synthesis of TiO_2, Fe-doped $TiO_2$and Ag-Fe co-doped TiO_2 nanocomposites

Nanoparticles can be prepared by different methods.[14] Amongst all, sol-gel method is simple, provides uniform size distribution and economical.[26] Nanoparticles were synthesized using a sol-gel synthesis method with little modification as this method provides anatase phase more after calcinations step which has more photocatalytic activity compared to amorphous and rutile

structure.[30-32] Fe content in nanoparticles were kept 0.5% by weight.[14,17,18] Fig. 1 represents steps for the synthesis of Ag-Fe co-doped TiO_2 nanoparticles. For the synthesis of Fe doped TiO_2, the $AgNO_3$ solution addition step was skipped. For the synthesis of TiO_2 nanoparticles, dopants were not added.

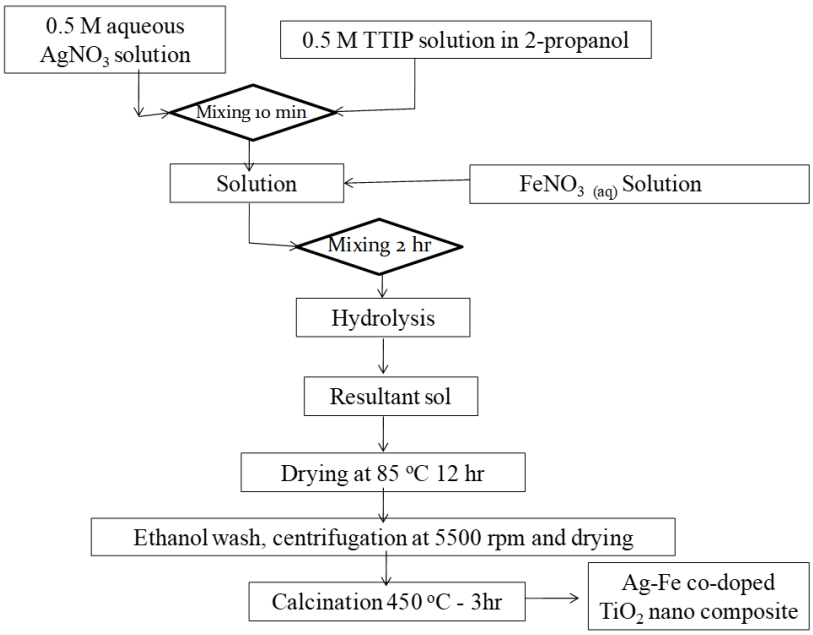

Fig. 1: Steps for the synthesis of nanoparticles

Characterization of Photocatalysts

Transmission Electron Microscopy (TEM) characterization was carried out using a JEOL JEM 2100 microscope operated at an acceleration potential of 200 kV.[36] Optical properties of the nanocatalysts were determined using the UV–Vis absorption spectroscopy with a Varian Cary 500, Shimadzu UV 3600. X-ray diffraction (XRD) analysis of the prepared photocatalysts was carried out at room temperature with a Philips: PW3040/60 XPERT Panalytical Pro using Cu K-alpha radiation (λ = 1.54 A) and a graphite monochromator, operated at 30 mA and 40 kV. The size and structure of synthesized photocatalysts were investigated using XRD and particle size analysis (Microtrack). From this study, considering the peak at 2θ degrees, average particle size was calculated by using equation (1) (Debye-Scherrer formula)[35-36]:

$$d = \frac{0.9\lambda}{\beta \cos\theta} \quad ...(1)$$

d: crystallite size (nm)
λ: wavelength of X-ray (0.154 nm)
β: FWHM (full width at half minimum)
θ: angle of diffraction (degrees)

A scanning electron microscope (SEM) was used to capture images to study the structure and surface of photocatalysts. The specific surface area was determined using BET Micromeritics, ASAP 2010. Elemental analysis was carried out with energy dispersive x-ray analysis (EDX) to verify the Ti/Ag molar ratio of the Ag-Fe CT 30.

Experimental Setup for Degradation of DFTA Under Solar and UV Light Irradiation

Fig. 2 represents solar photocatalysis experimental setup with a glass beaker as a reactor which was placed on magnetic stirrer to keep catalyst in suspension. The experiments were performed on terrace from 9 am to 2 pm and atmospheric air has worked as a natural oxidant for solar photocatalysis. Fig. 3 represents UV photocatalysis experimental set up with one closed chamber of 40 cm x 40 cm x 70 cm dimensions with a photocatalytic reactor of 800 ml capacity with a quartz tube to place UV light

surrounded by glass jacket for circulation of cooling water was used as shown in Fig. 3. UV radiations were provided using a 125 W UV lamp (wavelength, λ = 200-400 nm, Philips). The reaction mixture was magnetically stirred.

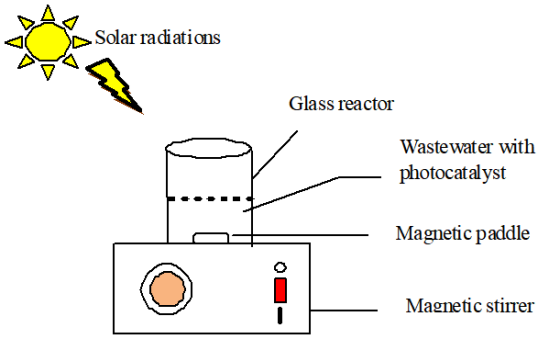

Fig. 2: Solar photocatalysis experimental setup

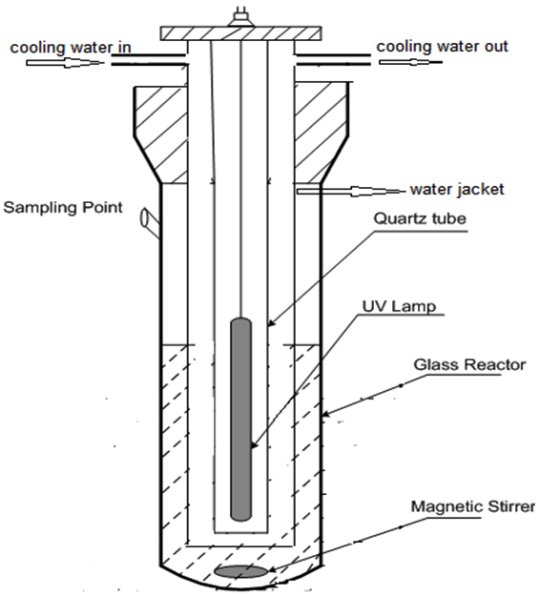

Fig. 3: UV photocatalysis experimental setup

Experimentation

A study on kinetics helps in the designing of photocatalytic reactors for the treatment of pharmaceutical wastewater. The reduction in the COD reflects the extent of mineralization of organic species.[39] Catalyst dose and pH were optimized by prior experiments for TiO_2, Fe TiO_2 and Ag-Fe CT 30 and were used for all the experiments. Amongst all commercial TiO_2, Digussa P25 TiO_2 has shown good photocatalytic activity and selected here for the study.[31,40,41] Photocatalysis for the degradation of DFTA were conducted batch wise using TiO2 C, synthesized TiO_2 np, Fe DT and Ag-Fe CT 30 under solar and UV light irradiation. The synthetic wastewater has an initial DFTA concentration of 8 g/L (COD_0 = 75520 mg/L) and the pH was maintained to 5 for Ag-Fe CT 30, 4 for Fe TiO_2 and 3 for TiO_2 using HNO_3. 3 g/L of Ag-Fe CT 30, 4 g/L of Fe TiO_2 and 5 g/L of TiO_2 as photocatalyst was added for photocatalysis. For UV photocatalysis externally oxygen is provided via air circulation through bubbler. 0.5 hr of irradiation time in dark was provided for adsorption of organics on catalyst surface before photocatalysis. Samples were extracted at an interval of 1 hr for a period of 6 hr for COD determination using the open reflux method. The samples were centrifuged at 5500 rpm to separate the catalyst from the solution before COD analysis for 5 min. The photocatalytic activity of TiO_2 C, TiO_2 np, Fe DT and Ag-Fe CT 30 photocatalysts in terms of COD removal efficiency were compared under UV and Solar light. All the experiments were carried out thrice to check reproducibility of the results and average values were considered. COD removal efficiency is calculated using equation (2).

$$\text{COD removal efficiency, \%} = \frac{COD0 - CODt}{COD0} * 100 \quad ...(2)$$

COD_0: initial chemical oxygen demand (mg/L)
CODt: chemical oxygen demand at time t (mg/L)

The recyclability of a photocatalyst is extremely important for practical applications.[25] Experiments were performed at optimized conditions repeatedly for six number of recycle runs to check the reusability of synthesized nanophotocatalysts under solar and UV radiations. At the end of first cycle, the used catalyst is separated from the solution and reused for the next consecutive six cycles hence total seven cycles have been performed. For regeneration of the photocatalyst, it was centrifuged at 5500 rpm for 15 min to recover it and washed with ethanol three times to remove traces of organics adsorbed on the surface. Finally, the separated wet particles were dried at 80-90°C in an oven overnight. The remaining all six runs of photocatalysis were then performed with the same steps used in the first cycle.

Results and Discussions

Nanoparticles Characterization

X-ray diffractograms of the synthesized nanoparticles are shown in Fig. 4. These results indicate that there is no impurity found and for all plots, the major peak is found at diffraction angle $2\theta = 25.3$, which represents the anatase phase (JCPDS card no. 21-1272) without any indication of the rutile phase. Anatase structure of TiO_2 has been focused many times by researchers for photocatalysis as it has shown high photocatalytic activity.[42–44,45] The X-ray diffraction patterns of Ag-Fe codoped TiO_2 photocatalysts almost coincide with that of undoped TiO_2, which indicates the dispersion of Ag and Fe on the TiO_2 surface. The results of particle size analysis (Fig. 5) show that the size of all the synthesized photocatalysts was between 10-30 nm. Fig. 6 represents UV-Vis spectra of different photocatalysts. It can be seen that Fe DT and Ag-Fe CT 30 can absorb visible irradiation due to the presence of Ag and Fe dopant.

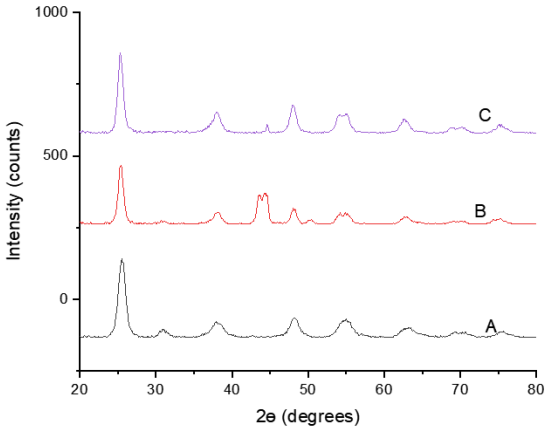

Fig. 4: XRD pattern of nanophotocataysts: A. TiO_2 np; B. Fe-doped TiO_2; C. Ag-Fe CT 30

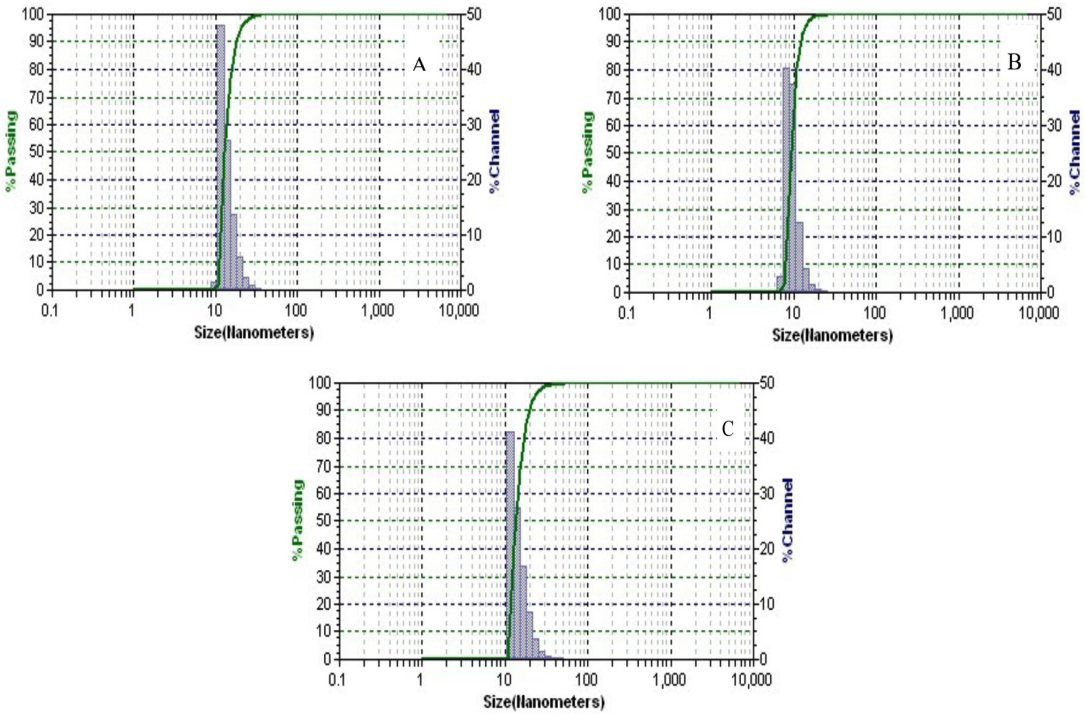

Fig. 5: distribution in nanophotocataysts: A. TiO_2 np; B. Fe-doped TiO_2; C. Ag-Fe CT 30

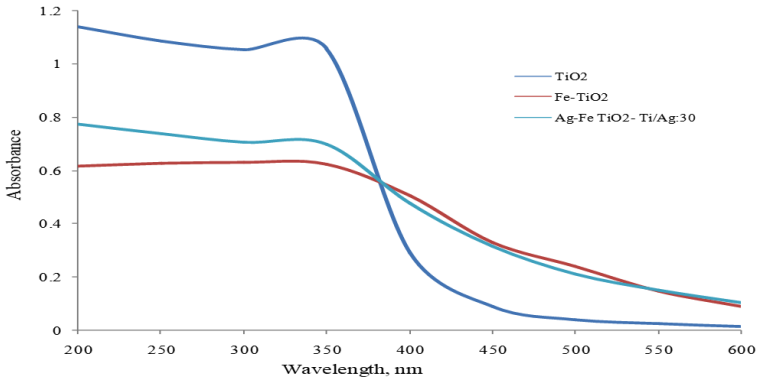

Fig. 6: UV-Vis spectra nanophotocatalysts

Morphology of Different Nanophotocatalysts

Fig. 7 represents SEM images of TiO_2 np, Fe DT and Ag-Fe CT 30. Results show that the TiO_2 nanophotocatalysts have a spherical shape with even surface, while the Fe-doped TiO_2, as well as Ag-Fe co-doped TiO_2, have spherical shape with irregular surface, indicating deposition of metal dopants on the surface of the TiO_2. TEM images of all synthesized photocatalysts are shown in Fig. 8. BET analysis indicated the maximum surface area of 760 m^2/g for Ag-Fe CT 30. Band gap was calculated from XRD peak data. Table 1 and Table 2 represent EDX elemental analysis and summary of characterization results respectively.

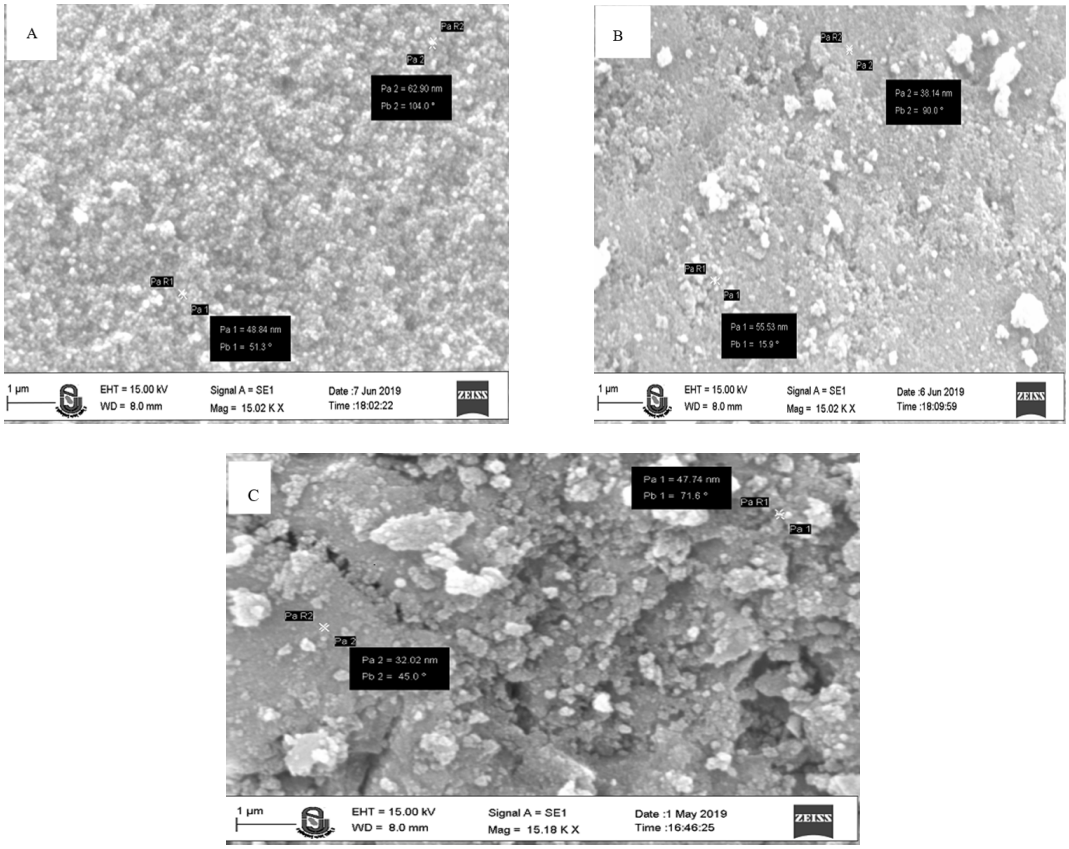

Fig. 6: SEM results of photocatalysts: A. TiO_2; B. Fe-doped TiO2; C. Ag-Fe CT 30

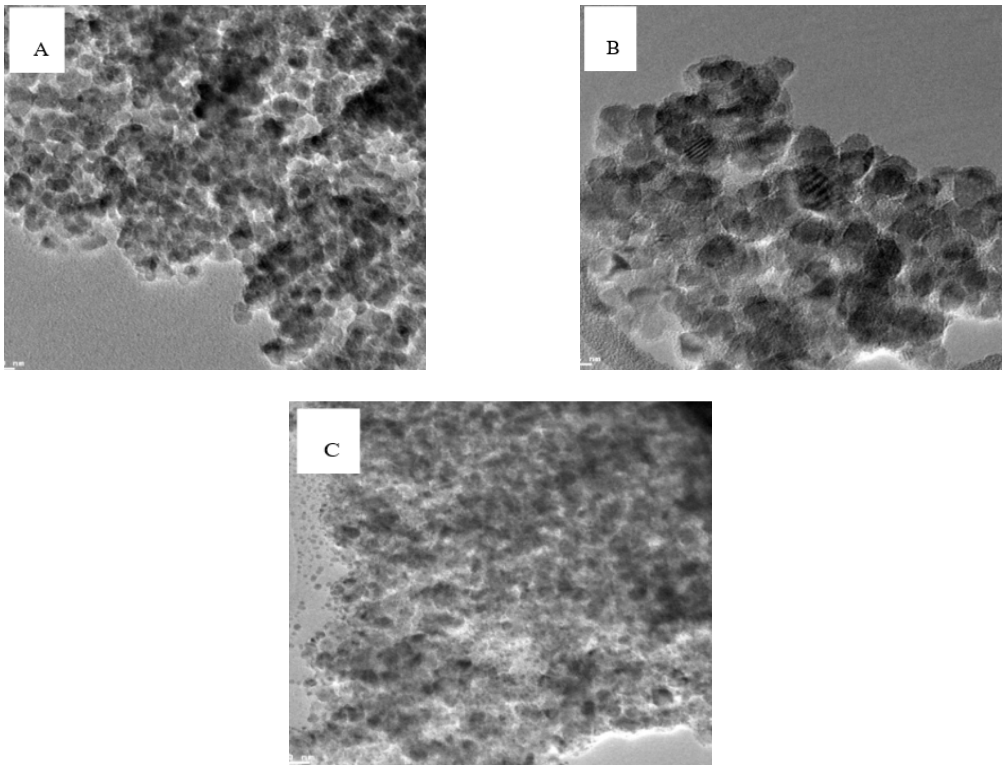

Fig. 8: TEM images of different photocatalysts: A. TiO_2 np; B. Fe-doped TiO2; C. Ag-Fe CT 30

Table 1: Calculation of Ti/Ag molar ratio for different nanophotocatalysts from EDX

Element	TiO_2	$FeTiO_2$	Ag-Fe co-doped nanophotocatalysts, wt%				
			Ti/Ag: 10	**Ti/Ag: 25**	**Ti/Ag: 30**	**Ti/Ag: 40**	**Ti/Ag: 55**
Ag	--	--	10.18	4.46	3.5	3.11	1.93
Ti	63.19	58.65	54.59	51.99	53.03	60.63	51.91
O	35.63	40.63	31.64	39.34	41.01	35.02	42.01
N	--	--	2.47	3.17	1.16	0	0
AuM	1.19	0.73	1.12	1.04	1.3	1.24	0.71
Total	100	100	100	100	100	100	100
Actual Ti/Ag molar ratio	-	-	11.97	26.03	33.81	43.52	60.05

Table 2: Summary of characterization results

Photocatalyst	Structure	Size from XRD, nm	Ti/Ag molar ratio from EDX	BET surface area, m2/g	Band gap, eV
TiO_2 np	Anatase	14.11	--	132.21	3.54
Fe DT	Anatase	12.90	--	94.22	3.35
Ag-Fe CT 30	Anatase	12.74	33.81	706.17	3.35

Photocatalytic Degradation of DFTA Using Different Photocatalysts

The COD removal efficiency with Ag-Fe CT 30 as a photocatalyst was compared with TiO2 C, TiO_2 np and Fe doped TiO_2 based on the COD reduction efficiency under solar and UV light at initial concentration of DFTA, 8 g/L, and at pH 5. In all the experiments, Ag-Fe CT 30 dose of 3 g/L for solar photocatalysis and UV photocatalysis was used. Ag-Fe CT has shown maximum COD removal efficiency under solar radiations due to following reasons: 1) OH radicals generation in large quantity by the combination of photocatalysis and fenton reactions due to presence of Ag and Fe dopants; 2) inhibition of electron and hole recombination as electrons might get trapped in doped metals results in separation of electron and holes thereby enhancing photocatalytic activity; 3) absorption of visible light due to presence of Ag and Fe dopants. The formation of reactive species such as H_2O_2, O_2^-, and OH* during photocatalysis will also oxidize DFTA. After 5 hr of irradiation time the COD removal efficiency was 37.77%, 63.09%, 52.79% and 85.54% under UV irradiations; 27.9%, 59.75%, 63.83% and 76.39% under solar irradiations respectively as shown in Fig. 9.

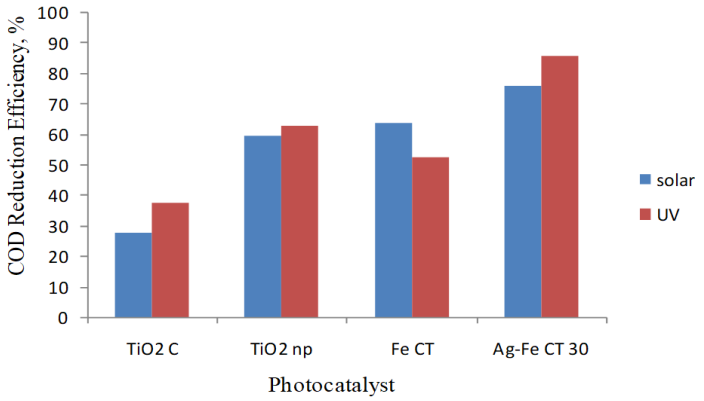

Fig. 9: Comparison of COD reduction efficiency under solar and UV radiations at optimum conditions

Kinetics of COD Removal for Solar and UV Photocatalysis Using Ag-Fe CT 30

Evaluation of parameters involved in the kinetic equation of COD removal is very important to study the effect of time on COD removal and thereby determination of volume requirement for the design of photocatalytic reactors. So, the kinetics of COD removal was calculated at initial DFTA concentration of 8 g/L, catalyst dose of 3 g/L and pH of 5 under solar and UV radiations. To evaluate the heterogeneous photocatalytic reaction successfully, the effect of COD remaining on the rate of COD removal rate is given in the form of equation (3).

$$-r = k * Cn \quad ...(3)$$
$$\log(-r) = n \log C + \log k$$

where (-r) is the COD removal rate, C is the COD at time 't', k is the rate constant, n is order of degradation reaction. To determine the parameters of equation (3), differential method of analysis was used. The rates of COD removal with COD remaining were obtained from plots of COD versus time data. COD versus time is plotted (Fig. 10 (a) and (c)) and values of n and k were calculated from the slope and intercept (Fig. 10 (b) and (d)) respectively. The rate constant and order obtained for solar and UV photocatalysis are shown in Table 3.

The rate of COD removal with the catalyst under solar light was higher than UV light, whereas maximum COD reduction of 87% was achievable during the fifth hour of UV photocatalysis which was higher than solar photocatalysis (76.74%) due to higher surface area and generation of OH radicals in abundance due to oxygen defects. The results higher rate under solar photocatalysis for such a high strength COD wastewater has proved its effectiveness for practical applications with economic and environmental benefits to the pharmaceutical industries.

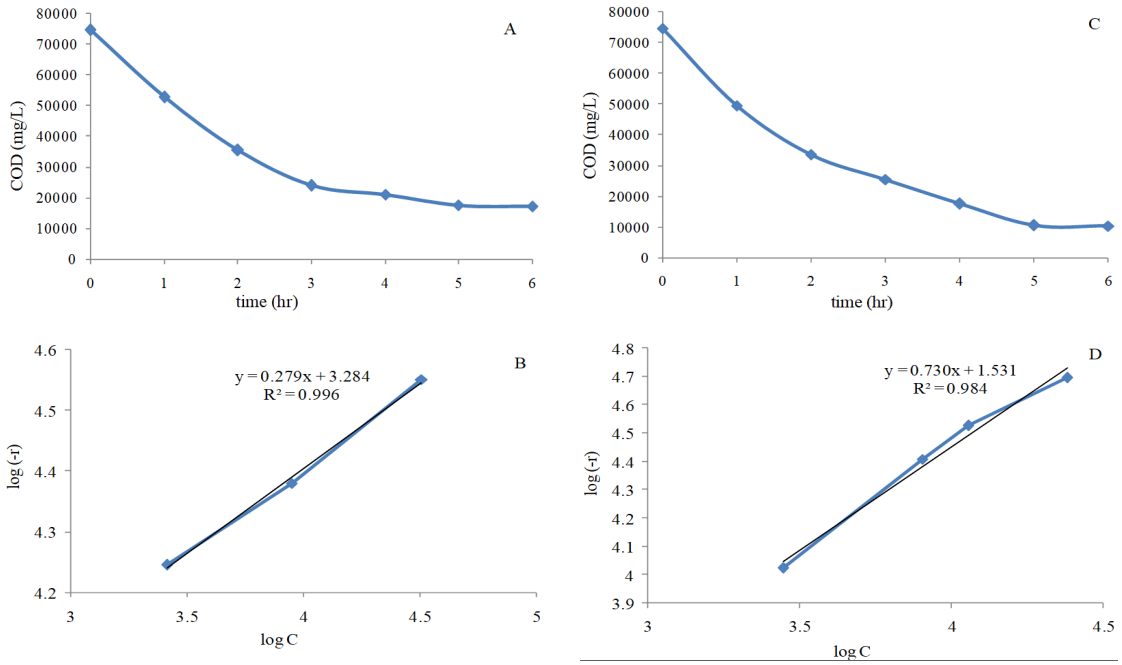

Fig. 10: Plot for kinetics of COD reduction efficiency using Ag-Fe CT as catalyst at conditions: pH = 5 and catalyst dose = 3 g/L (a) and (b) solar light; (c) and (d) UV light

Table 3 kinetic parameters for COD removal efficiency

	UV photocatalysis		Solar photocatalysis	
	Rate constant, hr^{-1}	**Order of reaction**	**Rate constant, hr^{-1}**	**Order of reaction**
	33.88	0.79	1905	0.28

Effect of Recycling of Ag-Fe CT 30

Fig. 11 shows % COD removal efficiency for 1 to 7 runs after 5 hr of irradiation under solar irradiations. After four cycles of reuse, decrease in photocatalytic activity of 5.88%, 8.7%, 6.62% and 4.86% for TiO_2 C, TiO_2 np, Fe DT, Ag-Fe CT 30 respectively were observed under solar light irradiation. With consecutive runs, the photocatalytic treatment efficiency dropped due to poisoning of catalyst and blockage of effective surface available for adsorption and oxidation reactions. The catalyst can be reused the four recycle runs without much decline in COD removal efficiency (less than 5%). 63.25% COD removal was even achievable by the novel Ag-Fe CT 30 during the sixth recycle run. The reuse efficiency was found to decrease in the following order for different photocatalysts: Ag-Fe CT 30>Fe DT>TiO_2 np>TiO_2 C. Ag-Fe CT 30 has proved its recyclability under solar radiations which makes effluent treatment economical and environmentally free as the treated effluent will not contain slight catalyst traces in discharged effluent. Recyclability of doped TiO_2 has been studied by various researchers and obtained nearly similar results.[43-44] Fe^{3+} doped TiO_2 was studied for dye degradation and there has been 9% reduction in degradation efficiency observed at the end of sixth cycle.[15] Ag/Fe,N-TiO_2/Fe_3O_4@SiO_2 and graphene oxide supported Ag-Fe TiO_2 has also shown good stability for visible light photocatalytic degradation of dyes for 5 and 3 recycle runs respectively.[45-46]

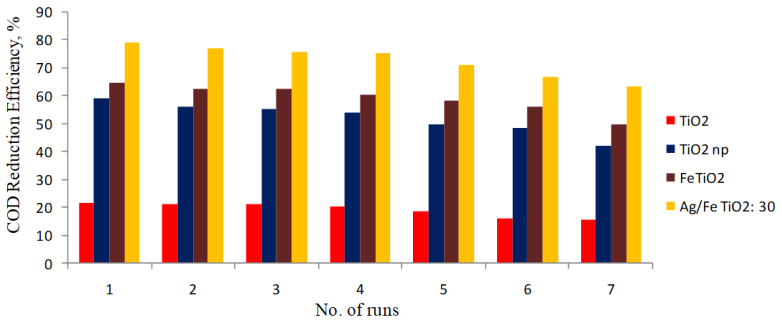

Fig. 11: Effect of catalyst recycling on percentage COD reduction efficiency

Industrial Wastewater Treatment at Optimized Conditions by Solar Photocatalysis

Batch photocatalysis experiments were performed with pharmaceutical industrial effluent having initial COD of 88660 mg/L and ammonical nitrogen (NH_3-N) of 3287 mg/L as specified in Table 4, under 5 hr (from 10 a.m. to 3 p.m) solar light irradiation and at the optimized conditions of pH and catalyst dose obtained for TiO_2, Fe DT and Ag-Fe CT 30. The optimum conditions for DFTA degradation by solar photocatalysis were: pH=3, catalyst dose= 3 g/L for TiO_2; pH=4, catalyst dose= 4 g/L for Fe DT; pH=5, catalyst dose= 3 g/L for Ag-Fe CT 30 and adsorption time in dark= 30 min under solar light. In all the experiments 500 mL volume of the industrial effluent was used. Fig. 12 shows the percentage removal of COD and NH_3-N from the effluent, obtained at the end of 5 hr at optimum conditions. Results of COD reduction showed that the synthesized catalyst worked efficiently for actual industrial wastewater treatment for COD reduction. Ag-Fe CT 30 has removed COD of effluent from 88660 mg/L to 31310 mg/L, 64.69% COD reduction. Since acidic conditions favor Organic oxidation and alkaline conditions favor NH_3-N reduction[50,51] simultaneous removal is not possible. Only 16.05% of NH_3-N could be removed during photocatalysis.

Table 4: Industrial wastewater treatment for COD and NH_3-N removal using solar photocatalysis

Parameter	Initial, mg/L	After treatment					
		TiO_2	% removal	Fe DT	% removal	Ag-Fe CT 30	% removal
COD, mg/L	88660	51460	41.96	45260	48.95	31310	64.69
NH_3-N, mg/L	3287	2960.58	9.93	2819.6	14.22	2760.24	16.03

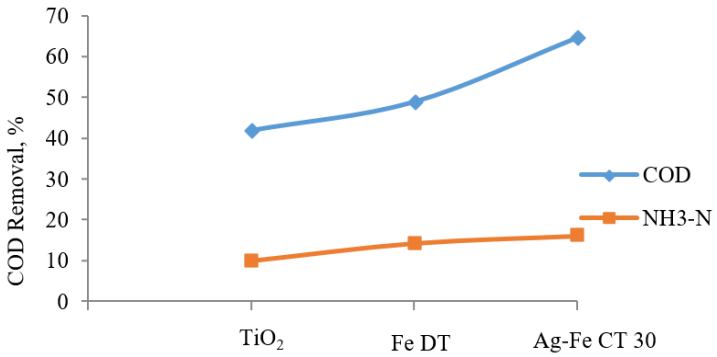

Fig. 12: COD and NH3-N removal from industrial wastewater using solar photocatalysis

Conclusion

A novel and efficient photocatalyst, Ag-Fe codoped TiO_2 with Ti/Ag molar ratio 30 was synthesized by the sol-gel method and its photocatalytic activity was compared with undoped TiO_2 for the photocatalytic degradation of DFTA, a drug intermediate. For economical operation, an attempt has been made to treat industrial pharmaceutical effluent with very high initial COD of 88660 mg/L under solar radiations using optimum conditions of pH and catalyst dose. Kinetics of COD removal favors photocatalysis under solar radiation compared to UV photocatalysis. Rate of solar photocatalysis is higher than UV photocatalysis during the first four hours with Ag-Fe CT 30 nanoparticles.

Acknowledgment

Authors thank VVP Engineering College, Gujarat Technological University and Gujarat Council of Science and Technology, Government of India, Gujarat for providing the financial support to carry out this research work.

Funding

The author(s) received no financial support for the research, authorship, and/or publication of this article.

Conflict of Interest

The authors do not have any conflict of interest.

References

1 A. M. Gutierrez, T. D. Dziubla, and J. Z. Hilt, "Recent advances on iron oxide magnetic nanoparticles as sorbents of organic pollutants in water and wastewater treatment," *Reviews on Environmental Health*, vol. 32, no. 1–2. Walter de Gruyter GmbH, pp. 111–117, 01-Mar-2017.

2 M. I. Khan e*t al.,* "Potential of Saudi natural clay as an effective adsorbent in heavy metals removal from wastewater," 2019.

3 C. Martinez-Boubeta and K. Simeonidis, "Magnetic Nanoparticles for Water Purification," in Nanoscale Materials in Water Purification, Elsevier, 2018, pp. 521–552.

4 R. H. Hesas, M. S. Baei, H. Rostami, J. Gardy, and A. Hassanpour, "An investigation on the capability of magnetically separable Fe3O4/ mordenite zeolite for refinery oily wastewater purification," *J. Environ. Manage.*, vol. 241, pp. 525–534, Jul. 2019.

5 N. A. Nahyoon *et al.,* "Significant photocatalytic degradation and electricity generation in the photocatalytic fuel cell (PFC) using novel anodic nanocomposite of Fe, graphene oxide, and titanium phosphate," *Electrochim.* Acta, vol. 271, pp. 41–48, May 2018.

6 M. Iqbal *et al.,* "Photocatalytic degradation of organic pollutant with nanosized cadmium sulfide," *Mater. Sci. Energy Technol.,* vol. 2, no. 1, pp. 41–45, Apr. 2019.

7 M. Iqbal et al., "Synthesis and characterization of transition metals doped CuO nanostructure and their application in hybrid bulk heterojunction solar cells," *SN Appl. Sci.*, vol. 1, no. 6, pp. 1–8, Jun. 2019.

8 Z. Ali, M. Mehmood, J. Ahmed, A. Majeed, and K. H. Thebo, "CVD grown defect rich-MWCNTs with anchored CoFe alloy nanoparticles for OER activity," *Mater. Lett.,* vol. 259, p. 126831, Jan. 2020.

9 M. Patel, R. Kumar, K. Kishor, T. Mlsna, C. U. Pittman, and D. Mohan, "Pharmaceuticals of emerging concern in aquatic systems: Chemistry, occurrence, effects, and removal methods," *Chemical Reviews,* vol. 119, no. 6. American Chemical Society, pp. 3510–3673, 27-Mar-2019.

10 V. D. Gosavi and S. Sharma, "Computer Science and Engineering & Technology An International Peer Review E-3 *Journal of Sciences and Technology* Available online at www.jecet.org Environmental Science Research Article JECET," 2013.

11 M. Yasmina, K. Mourad, S. H. Mohammed, and C. Khaoula, "Treatment heterogeneous photocatalysis; Factors influencing the photocatalytic degradation by TiO_2," in *Energy Procedia*, 2014, vol. 50, pp. 559–566.

12 N. C. Birben *et al.*, "Application of Fe-doped TiO_2 specimens for the solar photocatalytic degradation of humic acid," *Catal. Today*, vol. 281, pp. 78–84, Mar. 2017.

13 A. Nezamzadeh-Ejhieh and Z. Ghanbari-Mobarakeh, "Heterogeneous

photodegradation of 2,4-dichlorophenol using FeO doped onto nano-particles of zeolite P," *J. Ind. Eng. Chem.*, vol. 21, pp. 668–676, Jan. 2015.

14 Q. Chen *et al.,* "Enhancing the photocatalytic and antibacterial property of polyvinylidene fluoride membrane by blending Ag–TiO_2 nanocomposites," *J. Mater. Sci. Mater. Electron.,* vol. 28, no. 4, pp. 3865–3874, Feb. 2017.

15 F. Han, V. S. R. Kambala, R. Dharmarajan, Y. Liu, and R. Naidu, "Photocatalytic degradation of azo dye acid orange 7 using different light sources over Fe^{3+} doped TiO_2 nanocatalysts," *Environ. Technol. Innov.,* vol. 12, pp. 27–42, Nov. 2018.

16 Z. Chen and M. L. Fu, "Recyclable magnetic Fe^3O_4@SiO_2/β-$NaYF:Yb^{3+}$,Tm^{3+}/TiO_2 composites with NIR enhanced photocatalytic activity," *Mater. Res. Bull.,* vol. 107, pp. 194–203, Nov. 2018.

17 M. A. Farhan, Z. H. Mahmoud, and M. S. Falih, "Synthesis and characterization of TiO_2/Au nanocomposite using UV-Irradiation method and its photocatalytic activity to degradation of methylene blue," *Asian J. Chem.,* vol. 30, no. 5, pp. 1142–1146, 2018.

18 C. Girginov, P. Stefchev, P. Vitanov, and H. Dikov, "Silver doped TiO_2 photocatalyst for methyl orange degradation," *J. Eng. Sci. Technol. Rev.,* vol. 5, no. 4, pp. 14–17, 2012.

19 I. E. Paulauskas *et al.,* "Photocatalytic activity of doped and undoped titanium dioxide nanoparticles synthesised by flame spray pyrolysis," *Platinum Metals Review,* vol. 57, no. 1. pp. 32–43, 01-Jan-2013.

20 W. L. Wang and C. S. Yang, "Silver nanoparticles embedded titania nanotube with tunable blue light band gap," *Mater. Chem. Phys.,* vol. 175, pp. 146–150, Jun. 2016.

21 T. Ivanova, A. Harizanova, T. Koutzarova, and B. Vertruyen, "Optical and structural characterization of TiO_2 films doped with silver nanoparticles obtained by sol-gel method," *Opt. Mater. (Amst).,* vol. 36, no. 2, pp. 207–213, Dec. 2013.

22 F. Bensouici, T. Souier, A. A. Dakhel, A. Iratni, R. Tala-Ighil, and M. Bououdina, "Synthesis, characterization and photocatalytic behavior of Ag doped TiO_2 thin film," *Superlattices Microstruct.,* vol. 85, pp. 255–265, Jun. 2015.

23 M. Xia *et al.,* "Enhanced surface photovoltaic properties of TiO_2 nanowires doped by Ag nanoparticles," *Materials Letters*, vol. 160. Elsevier B.V., pp. 544–546, 24-Aug-2015.

24 G. Zhou *et al.,* "Surface plasmon resonance-enhanced solar-driven photocatalytic performance from Ag nanoparticles-decorated Ti^{3+} self-doped porous black TiO_2 pillars," *J. Ind. Eng. Chem.,* vol. 64, pp. 188–193, Aug. 2018.

25 D. Komaraiah, E. Radha, N. Kalarikkal, J. Sivakumar, M. V. Ramana Reddy, and R. Sayanna, "Structural, optical and photoluminescence studies of sol-gel synthesized pure and iron doped TiO_2 photocatalysts," *Ceram. Int.,* vol. 45, no. 18, pp. 25060–25068, Dec. 2019.

26 B. Cui, H. Peng, H. Xia, X. Guo, and H. Guo, "Magnetically recoverable core-shell nanocomposites γ-Fe_2O_3@SiO_2@TiO_2-Ag with enhanced photocatalytic activity and antibacterial activity," *Sep. Purif. Technol.,* vol. 103, pp. 251–257, 2013.

27 F. Petronella *et al.,* "Multifunctional TiO_2/FexOy/Ag based nanocrystalline heterostructures for photocatalytic degradation of a recalcitrant pollutant," *Catal. Today*, vol. 284, pp. 100–106, 2017.

28 Y. Chi *et al.,* "Magnetically separable Fe_3O_4@SiO_2@TiO_2-Ag microspheres with well-designed nanostructure and enhanced photocatalytic activity," *S* vol. 262, pp. 404–411, Nov. 2013.

29 A. Khanna and V. Shetty K, "Solar light-driven photocatalytic degradation of Anthraquinone dye-contaminated water by engineered Ag@TiO_2 core–shell nanoparticles," Desalin. *Water Treat.,* vol. 10, no. 3, pp. 376–385, 2014.

30 Z. Xiu *et al.,* "Recent advances in Ti^{3+} self-doped nanostructured TiO_2 visible light photocatalysts for environmental and energy applications," *Chemical Engineering Journal*. Elsevier B.V., 15-Feb-2019.

31 J. He *et al.,* "Facile Formation of Anatase/Rutile TiO2 Nanocomposites with Enhanced Photocatalytic Activity," *Molecules*, vol. 24, no. 16, p. 2996, Aug. 2019.

32 A. Giampiccolo et al., "Sol gel graphene/TiO_2 nanoparticles for the photocatalytic-assisted sensing and abatement of NO_2," *Appl. Catal. B Environ.,* vol. 243, pp. 183–194, Apr. 2019.

33 S. Sood, A. Umar, S. K. Mehta, and S. K. Kansal, "Highly effective Fe-doped TiO_2 nanoparticles photocatalysts for visible-light driven photocatalytic degradation of toxic organic compounds," *J. Colloid Interface Sci.,* vol. 450, pp. 213–223, Jul. 2015.

34 M. Crisan *et al.,* "Sol-gel iron-doped TiO<inf>2</inf> nanopowders with photocatalytic activity," *Appl. Catal. A Gen.,* vol. 504, pp. 130–142, Sep. 2015.

35 M. Safari, R. Talebi, M. H. Rostami, M. Nikazar, and M. Dadvar, "Synthesis of iron-doped TiO_2 for degradation of reactive Orange16," *J. Environ. Heal. Sci. Eng.,* vol. 12, no. 1, 2014.

36 B. Xin, L. Jing, Z. Ren, B. Wang, and H. Fu, "Effects of simultaneously doped and deposited Ag on the photocatalytic activity and surface states of TiO_2," *J. Phys. Chem. B*, vol. 109, no. 7, pp. 2805–2809, Feb. 2005.

37 J. Zhu, F. Chen, J. Zhang, H. Chen, and M. Anpo, "Fe^{3+}-TiO_2 photocatalysts prepared by combining sol-gel method with hydrothermal treatment and their characterization," *J. Photochem. Photobiol. A Chem.,* vol. 180, no. 1–2, pp. 196–204, May 2006.

38 H. Smail, M. Rehan, K. Shareef, Z. Ramli, A.-S. Nizami, and J. Gardy, "Synthesis of Uniform Mesoporous Zeolite ZSM-5 Catalyst for Friedel-Crafts Acylation," *Chem Engineering*, vol. 3, no. 2, p. 35, Apr. 2019.

39 P. Bansal and A. Verma, "Applications of sunlight responsive Fe-Ag-TiO_2 composite incorporating in-situ dual effect for the degradation of pentoxifylline," *Mater. Sci. Eng. B Solid-State Mater. Adv. Technol.*, vol. 236–237, pp. 197–207, Oct. 2018.

40 D. C. Hurum, A. G. Agrios, K. A. Gray, T. Rajh, and M. C. Thurnauer, "Explaining the enhanced photocatalytic activity of Degussa P25 mixed-phase TiO2 using EPR," *J. Phys. Chem. B*, vol. 107, no. 19, pp. 4545–4549, May 2003.

41 N. Bouanimba, N. Laid, R. Zouaghi, and T. Sehili, "A Comparative Study of the Activity of TiO_2 Degussa P25 and Millennium PCs in the Photocatalytic Degradation of Bromothymol Blue," *Int. J. Chem. React. Eng.,* vol. 16, no. 4, Oct. 2018.

42 S. Wang, J. S. Lian, W. T. Zheng, and Q. Jiang, "Photocatalytic property of Fe doped anatase and rutile TiO_2 nanocrystal particles prepared by sol-gel technique," *Appl. Surf. Sci.,* vol. 263, pp. 260–265, Dec. 2012.

43 R. J. Tayade, P. K. Surolia, R. G. Kulkarni, and R. V. Jasra, "Photocatalytic degradation of dyes and organic contaminants in water using nanocrystalline anatase and rutile TiO_2," *Sci. Technol. Adv. Mater.,* vol. 8, no. 6, pp. 455–462, Sep. 2007.

44 S. D. Delekar, H. M. Yadav, S. N. Achary, S. S. Meena, and S. H. Pawar, "Structural refinement and photocatalytic activity of Fe-doped anatase TiO_2 nanoparticles," *Appl. Surf. Sci.,* vol. 263, pp. 536–545, Dec. 2012.

45 K. M. S. H. M. Nagaveni, "Photocatalytic degradation of various dyes by combustion synthesized nano anatase TiO_2," *Appl. Catal. B Environ.,* vol. 45, no. 1, pp. 23–28, 2003.

46 C. Li, J. Tan, X. Fan, B. Zhang, H. Zhang, and Q. Zhang, "Magnetically separable one dimensional Fe_3O_4/P(MAA-DVB)/TiO_2 nanochains: Preparation, characterization and photocatalytic activity," *Ceram. Int., vol.* 41, no. 3, pp. 3860–3868, Apr. 2015.

47 M. B. Suwarnkar, R. S. Dhabbe, A. N. Kadam, and K. M. Garadkar, "Enhanced photocatalytic activity of Ag doped TiO_2 nanoparticles synthesized by a microwave assisted method," *Ceram. Int.,* vol. 40, no. 4, pp. 5489–5496, May 2014.

48 J. He, X. Zeng, S. Lan, and I. M. C. Lo, "Reusable magnetic Ag/Fe, N-TiO_2/Fe_3O_4@SiO_2 composite for simultaneous photocatalytic disinfection of *E. coli* and degradation of bisphenol A in sewage under visible light," *Chemosphere*, vol. 217, pp. 869–878, Feb. 2019.

49 D. P. Jaihindh, C. C. Chen, and Y. P. Fu, "Reduced graphene oxide-supported Ag-loaded Fe-doped TiO_2 for the degradation mechanism of methylene blue and its electrochemical properties," *RSC Adv., vol.* 8, no. 12, pp. 6488–6501, 2018.

50 D. Sun, W. Sun, W. Yang, Q. Li, and J. K. Shang, "Efficient photocatalytic removal of aqueous NH_{4+}-NH_3 by palladium-modified nitrogen-doped titanium oxide nanoparticles under visible light illumination, even in weak alkaline solutions," *Chem. Eng. J.,* vol. 264, pp. 728–734, Mar. 2015.

51 X. Luo *et al.,* "Characterization of La/Fe/TiO_2 and its photocatalytic performance in ammonia nitrogen wastewater," *Int. J. Environ. Res. Public Health*, vol. 12, no. 11, pp. 14626–14639, Nov. 2015.